Physica D 58 (1992) 10–30
North-Holland

PHYSICA D

Power spectra of noise-driven nonlinear systems and stochastic resonance

M.I. Dykman[1] and P.V.E. McClintock
School of Physics and Materials, Lancaster University, Lancaster, LA1 4YB, UK

Received 4 October 1991
Revised manuscript received 17 January 1992
Accepted 17 January 1992

The results of recent experimental and theoretical investigations of the spectral densities of fluctuations (SDFs) of noise-driven nonlinear dynamical systems are reviewed. Emphasis is placed on the analysis of the shapes and intensities of peaks in the SDFs. Three different types of phenomena are considered. First, the SDFs of a class of monostable underdamped nonlinear systems, in which the variation of eigenfrequency with energy is nonmonotonic, are investigated. It is shown that they exhibit zero-dispersion peaks and noise-induced spectral narrowing, as well as zero-frequency peaks. Secondly, it is demonstrated that systems bistable in an external periodic field can exhibit supernarrow spectral peaks within the range of a kinetic phase transition. Finally, recent results in stochastic resonance (SR) are reviewed, including phase shifts, giant nonlinearities for weak noise, SR for periodically modulated noise intensity, and high-frequency SR for periodic attractors.

1. Introduction

Spectral densities of fluctuations (SDFs) provide an important means of characterising physical systems, because they can be measured directly in a variety of experiments: in particular, the optical and neutron spectra of systems in thermal equilibrium (or quasiequilibrium) – one of the main sources of information about the microscopic characteristics of many such systems – are immediately related to SDFs. The investigation of SDFs also makes possible to observe and analyse the interplay between the fluctuations, relaxation and nonlinearity that are inherent to real macroscopic physical systems. This interplay provides one of the most challenging problems of modern nonlinear physics.

In many cases of interest, the physical system to be investigated can be modelled by a more or less complicated damped dynamical system that is subject to noise. If the noise and the relaxation are both due to coupling to a thermal bath, then they will satisfy the fluctuation-dissipation relations [1] and the characteristic intensity of the noise will be equal to the temperature T of the bath. In the general case, a nonthermal noise is also present. Certain properties of the systems and of their SDFs in particular, are highly sensitive to the characteristics of the noise, while others are universal and depend only weakly on these characteristics. Both types of property are clearly of importance in different contexts. In what follows, our main aim will be to consider *phenomena* exhibited by noise-driven archetypal models. Similar phenomena may of course then be predicted for real systems, over a very wide range of contexts in science and technology whenever they are described by equations of the same general form as those we will discuss.

[1] Now at: Department of Chemistry, Stanford University, Stanford, CA 94305, USA.

0167-2789/92/$05.00

In the present paper we outline recent results on the SDFs of relatively simple, although nontrivial, nonlinear systems. Emphasis is placed on the shapes and intensities of the peaks of the SDF. Three sorts of effects are considered. In section 2 we analyse the shapes of the peaks for monostable underdamped nonlinear systems and investigate effects related to nonmonotony of the dependence of the frequency of eigenvibrations $\omega(E)$ on the energy E of a system. Such nonmonotony is inherent in a number of vibrational systems. Examples include the localised vibrations in solids, where nonmonotony will arise provided that the "stiffness" of the system increases with energy for small E (see [2] for a review) and where it can be controlled by external electric field and/or pressure. For systems of this kind, the widths of the SDF peaks at first increase in the usual way with increasing noise intensity, relative to their low noise values (which are determined by damping). Surprisingly, however, they can sometimes *decrease* again, by a large factor, as the noise intensity continues to rise. Moreover, for very small damping, a specific zero-dispersion peak can arise at the frequency of the extremum [3].

In section 3 the SDF is investigated for bistable systems, with the emphasis on bistability arising in an external periodic field where the coexisting stable states correspond to forced periodic vibrations with different amplitudes and phases. Bistable systems driven by a sufficiently weak noise have a very large characteristic relaxation time that is given by the reciprocal probabilities of fluctuational transitions between the stable states. Associated with this time is an extremely small spectral width of the peaks of the SDF (supernarrow peaks) that arise at the frequency of the driving field and its overtones, and also at zero frequency. The peaks exhibit a critical-type behaviour for the parameters of the system lying in the vicinity of a kinetic "phase transition" where the stationary populations of the coexisting stable states are of the same order of magnitude.

In section 4 a phenomenon directly related to the aforementioned super-narrow peaks is investigated, namely, the onset of a strong response of a bistable noise-driven system to a comparatively weak (trial) periodic field [4] and the dome-like (bell-shaped) dependence of the response on the noise intensity called *stochastic resonance* by Benzi et al. [5] (see also [6]). This phenomenon has attracted considerable interest recently and has been observed in both active [7] and passive [8] optically bistable systems and also in analogue electronic experiments [9–12].

2. Noise-induced narrowing of the spectral peaks of monostable underdamped systems

In view of its importance and a wide variety of applications, the problem of the power spectra of nonlinear vibrational systems has been considered by many authors, both numerically and analytically (see refs. [13–24] and the reviews [4b, 25]). Underdamped systems, in particular, are of the utmost interest, because of their association with resonant phenomena, including, e.g. resonant light absorption and neutron scattering in condensed matter that is directly described just by the SDFs. It is generally accepted that the peaks of the SDF usually become substantially broader as the external noise intensity increases. This is due to the growth of fluctuations in the system. However, as is shown below, in some systems the broadening is followed, remarkably, by a narrowing of the peaks with further increase of the noise intensity.

We shall investigate evolution of the peaks for the simplest model of a fluctuating nonlinear system, a nonlinear oscillator performing Brownian motion. It is described by the equation

$$\ddot{q} + 2\Gamma\dot{q} + U'(q) = f(t)\,,$$
$$\langle f(t)\, f(t')\rangle = 4\Gamma T\delta(t - t') \tag{1}$$

If its fluctuations correspond to thermal equilibrium, then T in (1) is the temperature, whereas in the more general case it simply characterises the intensity of the driving noise which, in the present section, is supposed to be white and Gaussian. The damping Γ is assumed small,

$$\Gamma \ll \omega_0\,, \quad \omega_0 \equiv \omega(0) = [U''(q_{eq})]^{1/2}\,, \tag{2}$$

where $\omega(E)$ is the eigenfrequency of conservative vibrations with a given energy E,

$$E = \tfrac{1}{2}\,\dot{q}^2 + U(q) \tag{3}$$

(the energy is measured from the value of the potential $U(q)$ in the equilibrium position q_{eq}: $U(q_{eq}) = U'(q_{eq}) = 0$).

In what follows (see, however, section 4) we shall consider the SDF of the coordinate defined as

$$Q(\omega) = \lim_{t_0\to\infty} (4\pi t_0)^{-1} \times \left| \int_{-t_0}^{t_0} \mathrm{d}t\,[q(t) - \langle q(t)\rangle]\exp(\mathrm{i}\omega t)\right|^2 . \tag{4}$$

Here, $\langle\ldots\rangle$ implies the ensemble average (which is well known [1, 4b] to differ from the time average for the periodically driven systems considered below; for such systems the time axis is evidently "inhomogeneous").

2.1. Peak of the SDF for "small" noise intensities

For very weak noise (small T) the oscillator (1) can be assumed effectively harmonic, with an eigenfrequency ω_0 and damping parameter Γ. The SDF $Q(\omega)$ for such an oscillator is well known (cf. [1]) to have a Lorentzian peak at the frequency ω_0, with a halfwidth at halfmaximum just equal to Γ. With increasing noise intensity the shape of the peak changes, and this change can be strong even for relatively small noise intensities (which was probably noticed for the first time in ref. [26] where the quantum theory of the spectra of localised vibrations was considered).

The origin of the strong noise-induced broadening of the spectral peak can easily be understood from fig. 1. Because of fluctuations, a distribution of the oscillator is formed over the energy E. Its characteristic width is given by the driving-noise intensity T. In its turn, because of nonlinearity, this distribution gives rise to a distribution of the oscillator over the corresponding range of vibrational eigenfrequencies $\omega(E)$ i.e., there arises a noise-induced frequency straggling $\delta\omega_{fl}$ which for small noise intensities is equal to

$$\delta\omega_{fl} = T|\omega_0'|\,, \quad \omega_0' \equiv [\mathrm{d}\omega(E)/\mathrm{d}E]_{E=0}\,, \quad \delta\omega_{fl} \ll \omega_0\,. \tag{5}$$

The frequency straggling (5) "competes" with the frequency "uncertainty" Γ arising from damping. The shape of the peak in the SDF depends just on the ratio of these two quantities:

$$\alpha = \tfrac{1}{2}(\delta\omega_{fl}/\Gamma)\,\mathrm{sgn}\,\omega_0'\,.$$

For arbitrary α, but for both weak damping, $\Gamma \ll \omega_0$, and "weak" noise, $\delta\omega_{fl} \ll \omega_0$, the peak is

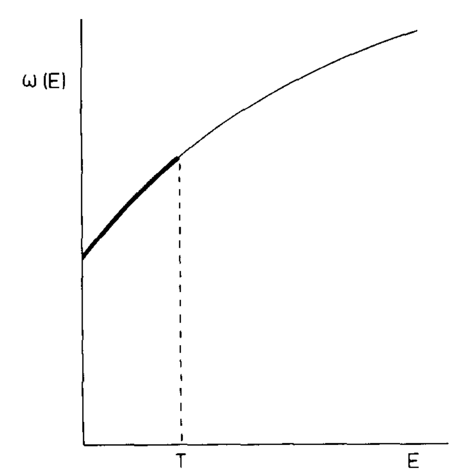

Fig. 1. Variation of eigenfrequency $\omega(E)$ with the energy E for a general nonlinear oscillator. If the oscillator is driven by noise of intensity T, its energy will be described by a distribution whose width is approximately equal to T, so that the frequencies of the thermally excited vibrations are mostly those on the thickened portion of the curve.

described by a comparatively simple expression [15]

$$Q(\omega) = \frac{T}{2\pi\omega_0^2} \operatorname{Re} \int_0^\infty \mathrm{d}t \exp[\mathrm{i}(\omega - \omega_0)t]\, \tilde{Q}^*(t)\,,$$

$$|\omega - \omega_0| \ll \omega_0\,,$$

$$\tilde{Q}(t) = \exp(\Gamma t) \times \left(\cosh(at) + \frac{\Gamma}{a}(1 - 2\mathrm{i}\alpha)\sinh(at)\right)^{-2},$$

$$a = \Gamma(1 - 4\mathrm{i}\alpha)^{1/2}\,. \tag{6}$$

It follows from (6) that for $|\alpha| \gg 1$, i.e. for $\delta\omega_{\mathrm{fl}} \gg \Gamma$ it is fluctuational broadening that determines the shape of the peak in the SDF near its maximum. It also follows that, in contrast to the case $|\alpha| \ll 1$ where $Q(\omega) \propto \Gamma T/[\Gamma^2 + (\omega - \omega_0)^2]$ is symmetrical near the maximum, for $|\alpha| \gg 1$ the peak is strongly asymmetric. The shape of the peak in the latter case can readily be understood by noting that the amplitude of the eigenvibrations increases with increasing energy (as $E^{1/2}$ for small E), while the probability of the system having an energy E decreases exponentially, according to the Gibbs law. The product of the squared amplitude times $\exp(-E/T)$ is "mapped" onto the spectral distribution $Q(\omega)$ via the relation $\omega = \omega(E) = \omega_0 + \omega_0' E$, so that $Q(\omega)$ near the maximum is proportional to $[(\omega - \omega_0)/\omega_0'] \exp[-(\omega - \omega_0)/\omega_0' T]$. The position of the maximum itself is given by $\omega_0 + T\omega_0' = \omega(T)$ and the peak increases rapidly in width with the noise intensity, being much steeper on the side of the sharp low-energy threshold (cf. fig. 1).

The above picture has been completely confirmed by analogue electronic experiments [24, 27]. The evolution of the SDF with increasing noise intensity for an oscillator (1) with the potential

$$U(q) = \tfrac{1}{2}q^2 + \tfrac{1}{4}q^4 + \lambda q \tag{7}$$

at $\lambda = 0$, when the eigenfrequency $\omega(E)$ increases monotonically with E, as observed in [27], is shown in fig. 2. The stronger the noise the broader the peak, and its width for the values of T in fig. 2 substantially exceeds the relaxational broadening Γ.

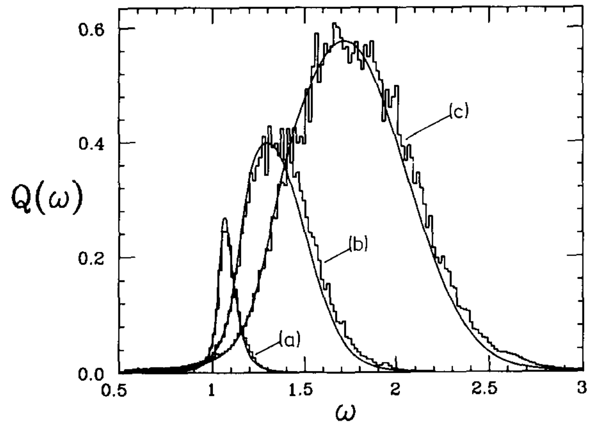

Fig. 2. Spectral density $Q(\omega)$ of the fluctuations of the oscillator described by (1) and (7) for damping $\Gamma = 0.0143$ and the asymmetry parameter $\lambda = 0$, as measured (histograms) in an analogue experiment [27] for comparison with theoretical predictions (curves), for noise intensities: (a) $T = 0.078$; (b) 0.687; (c) 3.04.

Strikingly similar behaviour has been observed [28] in the optical absorption spectra of localised and resonant vibrations in solids as shown, for example, by the results of fig. 3. Just as in the

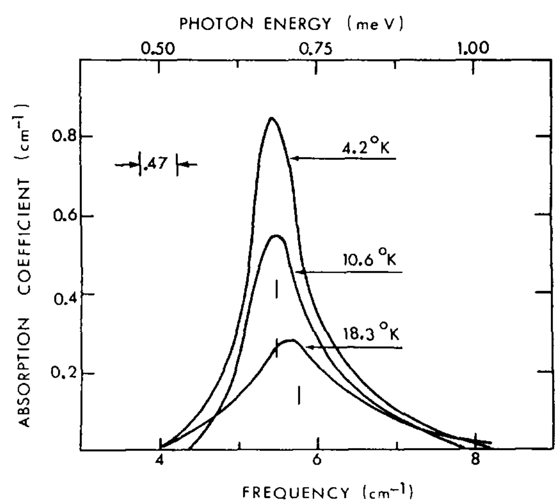

Fig. 3. Temperature dependence of the far-infrared absorption in an NaI crystal doped with 0.4% NaCl [28].

case of the Duffing oscillator SDFs of fig. 2, the absorption spectrum of the resonant mode in fig. 3 broadens rapidly and becomes noticeably asymmetric with increasing temperature. (The dependences of the intensity on temperature in the two graphs differ because the optical absorption cross-section in the experiment of fig. 3 varies approximately as the SDF divided by temperature.) We note that, in many physical systems, effects arising from quantum statistics (i.e. related to the discreteness of the energy levels) of the localised modes are important: such effects are beyond the scope of the present review.

2.2. *Noise-induced narrowing and onset of the zero-dispersion peak*

A peculiar situation of particular interest arises when the dependence of the eigenfrequency $\omega(E)$ on the vibration energy E is nonmonotonic and for some energy E the derivative $\omega'(E)$ passes through zero,

$$[\mathrm{d}\omega(E)/\mathrm{d}E]_{E=E_e} = 0\,, \quad \omega(E_e) \equiv \omega_e \tag{8}$$

(cf. fig. 4; for convenience in understanding the experimental data in figs. 2, 5 we have chosen in fig. 4 an initial slope $\omega_0' = [\mathrm{d}\omega(E)/\mathrm{d}E]_{E=0}$ that is opposite in sign to that in fig. 1, but which corresponds to the particular system considered below). If (8) is fulfilled there are two "cutoff" frequencies, ω_0 and ω_e. For small noise intensities, $T \ll E_e$, when the vibrations with the eigenfrequencies close to ω_e do not come into play, the behaviour of $Q(\omega)$ with increasing T is described by the results of the preceding subsection.

However, for T approaching E_e and the position of the maximum of $Q(\omega)$ approaching ω_e, respectively, the "flattening" of $\omega(E)$ becomes more and more marked. In essence, as is obvious from the above arguments, the peak of $Q(\omega)$ is "pressed" against the frequency ω_e: vibrations with higher and higher amplitudes are being excited, and their eigenfrequencies approach ω_e.

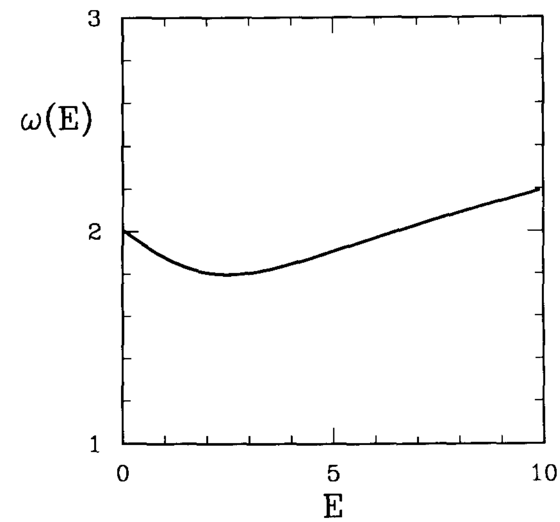

Fig. 4. Variation of eigenfrequency $\omega(E)$ with energy E for the particular oscillator described by (1), (7), with $\lambda = 2$. It is the existence of an extremum in $\omega(E)$ that is responsible for the noise-induced spectral narrowing and zero-dispersion spectral peaks discussed in the text.

But there are no eigenfrequencies beyond this cutoff. As a result the peak becomes narrower with increasing T and also becomes steeper on the ω_e-side, i.e. the exact opposite of the situation for small T.

Spectral narrowing was first observed in an analogue experiment and then described in detail theoretically [27]. The theory reduced the problem of calculating the peak of the SDF to a boundary-value problem for an ordinary differential equation related to the Fokker–Planck equation for a noise-driven oscillator: the former equation was a Fourier-transformed (over time) equation for diffusion in energy, but, in contrast to Kramer's paper [29], it was the equation not for the phase-independent, but for the phase-dependent (as $\exp(in\phi)$, with $|n| = 1$ in the present case) part of the distribution function.

The experimental and theoretical results for the model (1), (7), demonstrating the noise-induced narrowing of the spectral peak, are shown in fig. 5. We would note that the model (7) is extremely simple in that it contains only one control parameter λ which might be associ-

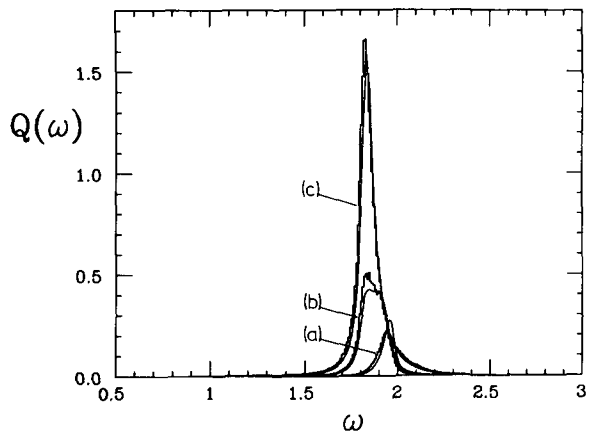

Fig. 5. Spectral densities $Q(\omega)$ of the fluctuations of the oscillator described by (1), (7) for $\Gamma = 0.0143$ and the asymmetry parameter $\lambda = 2$, as measured (histograms) in an analogue electronic experiment [27] for comparison with theoretical predictions (curves) for noise intensities: (a) $T = 0.078$; (b) 0.687; (c) 3.04. Note the narrowing of the width at the half-height as the noise intensity is increased between (b) and (c).

ated, e.g., with an electric field for an oscillating charged particle, or a static pressure. For $\lambda = 0$ the eigenfrequency $\omega(E)$ increases monotonically with E and there is no spectral narrowing (cf. fig. 2). The nonmonotony of $\omega(E)$ arises for $|\lambda| > 8/7^{3/2} \cong 0.43$, and starting with slightly higher $|\lambda|$ (because of finite damping; the data refers to $\Gamma \cong 0.015$) the nonmonotony of the peak width vs T was observed. The theory is evidently in excellent agreement with the experiment, and we would stress that it does not contain any adjustable parameter.

A very interesting phenomenon arises in systems with nonmonotonic $\omega(E)$ for still smaller damping Γ/ω_e [3]: the onset of an additional narrow peak in the SDF at the extreme frequency ω_e for sufficiently high noise intensities. Qualitatively, such a zero-dispersion peak arises because the system spends a relatively long time oscillating at frequencies close to ω_e: for $E \cong E_e$ fluctuations over energy have little effect on the frequency or phase of the eigenvibrations. The characteristic width $\delta\omega_{zd}$ of the peak can be readily obtained by noting that $\delta\omega_{zd}$ is due to the frequency diffusion over the time $\delta t \sim (\delta\omega_{zd})^{-1}$; in its turn, the frequency diffusion is due to energy diffusion over the time δt; $\delta E \sim (4\Gamma T I_e \omega_e \delta t)^{1/2}$ (cf. [29]), where I_e is the action for the vibrations with the energy E_e. Therefore,

$$\delta\omega_{zd} = (2\Gamma|\omega_e''| T I_e \omega_e)^{1/2} ,$$
$$\omega_e'' \equiv [\mathrm{d}^2\omega(E)/\mathrm{d}E^2]_{E_e} ,$$
$$I_e = \int_0^{E_e} \omega^{-1}(E)\, \mathrm{d}E . \tag{9}$$

We note that the change in frequency $\omega(E)$ over a time $(\delta\omega_{zd})^{-1}$ due to the drift in energy is of

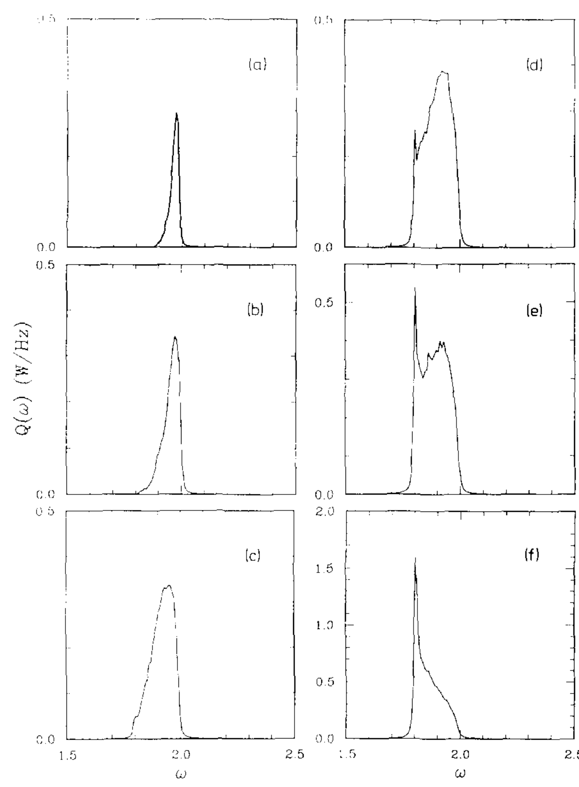

Fig. 6. Spectral densities $Q(\omega)$ of the fluctuations of an electronic model [30] of the oscillator described by (1), (7) for very small damping $2\Gamma = 1.70 \times 10^{-3}$ and the asymmetry parameter $\lambda = 2$, for several noise intensities: (a) $T = 0.100$; (b) 0.203; (c) 0.320; (d) 0.409; (e) 0.485; (f) 0.742. The zero-dispersion peak is the sharp "spike" that first appears in (d); it rapidly grows, overwhelming the usual spectral peak as T increases, in (f).

order $\omega_e''(\Gamma\omega_e I_e/\delta\omega_{zd})^2 \ll \delta\omega_{zd}$, and can thus be neglected, i.e. the broadening of the peak is purely diffusional. The shape of the zero-dispersion peak is described by the expression [3]

$$\delta Q_{zd}(\omega) = \text{const.} \times \exp(-E_e/T) \times |S[(\omega - \omega_e)\,\mathrm{sgn}(\omega_e'')/\delta\omega_{zd}]| ,$$
$$S(x) = \mathrm{Re}\int_0^\infty \mathrm{d}t \exp(-\mathrm{i}xt) \times [(1-\mathrm{i})\sinh((1-\mathrm{i})t)]^{-1/2} . \qquad (10)$$

Analogue simulations of the model (1), (7) have made it possible to reveal the zero-dispersion peak [30]. The evolution of the SDF with increasing temperature for very small damping, $\Gamma = 8.5 \times 10^{-4}$, is shown in fig. 6. It is obvious from this figure that the zero-dispersion peak emerges very suddenly with increasing temperature, and then grows rapidly to dominate the spectrum. The sharp "outburst" of the peak (due to the competition of the exponentially small occupation of the energies $E \sim E_e$ for small T and the sharpness of the peak itself) has recently been described analytically [31], and the theory has been demonstrated [30] to be in good agreement with the experiment.

2.3. Zero-frequency peaks in SDFs of monostable system

A well-known feature of nonlinear vibrations is that they are not strictly sinusoidal: in addition to the fundamental frequency $\omega(E)$ there also exist overtones $n\omega(E)$ $(n = 2, 3, \ldots)$ in their Fourier spectrum. It is to be expected, therefore, that in addition to the peak in the SDF corresponding to the main tone (see above) there will also be peaks corresponding to the overtones. Peaks of this sort have indeed been observed, e.g., in the absorption spectra of localized vibrations in solids [32] (see [2] for a review). Their width increases with the number n of the overtone (cf. [33]) and exceeds that for the main tone.

For an underdamped oscillator fluctuating in an asymmetric potential well there arises, in addition, a well-resolved comparatively narrow peak in the SDF at zero frequency [24, 34] (we note that for overdamped oscillators the peak at zero frequency is the only one in the spectrum). The quantum theory of a corresponding peak in the absorption spectra of weakly nonlinear localized vibrations was given in ref. [35].

The zero-frequency peak in the SDF of the coordinate q is related to the fact that, in asymmetric potential wells, the fluctuations of the oscillator energy E give rise to fluctuations of the *centre* of the vibrations with a given energy, $q_0(E)$. These fluctuations are "slow", with a characteristic time scale equal to the relaxation time Γ^{-1}. They are purely relaxational and are not associated with any finite frequency, and thus the corresponding SDF peak should be positioned at zero frequency and have a half-width of order Γ. A simple theory shows that, for small noise intensities, the shape of the zero-frequency peak is given by the expression [34]

$$Q_0(\omega) = \frac{1}{\pi} q_0'^2 T^2 \frac{2\Gamma}{4\Gamma^2 + \omega^2} \times \left[1 + 4T\left(\frac{q_0''}{q_0'} - \frac{4(\omega_0'/\omega_0)\Gamma^2}{4\Gamma^2 + \omega^2}\right)\right] ,$$
$$q_0' = [\mathrm{d}q_0(E)/\mathrm{d}E]_{E=0} ,$$
$$q_0'' = [\mathrm{d}^2 q_0(E)/\mathrm{d}E^2]_{E=0} \qquad (11)$$

An important feature of the zero-frequency peak is that it is not affected by the straggling of the frequencies of eigenvibrations induced by the combined effects of noise and nonlinearity (see above). Therefore it does not broaden rapidly with increasing noise intensity. It is because of this that the zero-frequency peak in the SDF is resolved much better than the peaks at the overtones: peaks of both types are due to nonlinearity of the vibrations, and therefore their intensities increase with noise strength, but the width of the zero-frequency peak becomes much smaller for noise strengths beyond $T \sim \Gamma/|\omega_0'|$ and, correspondingly, it is much higher. In addition, for relatively small noise, the intensity of the peak at the second overtone (the "main" overtone for weak noise) contains an extra numerical factor $\frac{1}{9}$ [33] compared to that of the zero-frequency peak. An overall view of the SDF for the oscillator (1), (7) as obtained for the relevant electronic model and described theoretically, with a clearly visible zero-frequency peak, is shown in fig. 7. The insert demonstrates that the broadening of this peak with increasing noise is indeed small and that sometimes, rather than broadening, noise-induced narrowing may occur; this follows from eq. (11).

In concluding this section, we note that the shape of the fundamental peak for not very weak noise, when the main broadening mechanism is the fluctuational one, reflects the stationary distribution of the system over its energy (the peak gives the "projection" of this distribution on the distribution over the frequencies $\omega(E)$). Therefore it is quite sensitive to the characteristics of the driving noise, whereas the shape of the zero-frequency peak is much less sensitive to these characteristics.

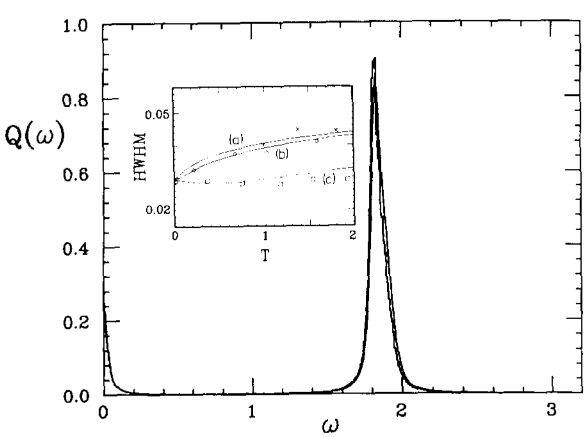

Fig. 7. Spectral density $Q(\omega)$ of the fluctuations of the oscillator described by (1), (7) for damping $\Gamma = 0.0143$ and with the asymmetry parameter $\lambda = 2.0$, for a noise intensity $T = 0.814$. The full spectrum (except for the overtones) is plotted, with the zero-frequency peak on the left-hand side and the peak corresponding to eigenvibrations at the fundamental frequency on the right-hand side. The histogram represents data from an electronic model, and the full curve represents the theory [34]. Inset: the variation of the width (defined as the half-width at half-maximum) of the zero-frequency peak, as a function of noise intensity T for three values of the asymmetry parameter: (a) $\lambda = 0.2$; (b) 0.43; (c) 2.0. The data points represent measurements on the electronic model, and the full curves represent the theory.

3. Super-narrow spectral peaks in the SDFs of bistable systems

Many physical systems of particular interest have not one, but two or more coexisting attractors. These may be potential minima for a diffusing particle (e.g., for an impurity in a solid, or a reorientating molecule) or coexisting regimes of laser generation, passive optical transmission, or forced oscillations of an electron in a Penning trap [36], etc. A quite general feature of fluctuations in bistable (or multistable) systems is that, in addition to the relaxation time (times) τ_{rel} characterising the dynamics in close vicinity to one of the attractors, the fluctuations are also characterised by much larger times associated with the noise-induced transitions between the attractors. These are equal to the reciprocal transition probabilities W_{ij}^{-1} (i, j enumerate the attractors, i, $j = 1, 2$). For a broad class of systems driven by Gaussian noise the dependence of W_{ij} on the characteristic noise intensity D is of the activation type (see [4, 37–41] and references therein),

$$W_{ij} = \text{const.} \times \exp(-R_i/D) . \tag{12}$$

Here, R_i can be associated with the activation energy of the transition from the state i (in Kramers' model [29] of the activation of a Brownian particle over a potential barrier, R_i is the height of the barrier and D is the temperature). It is obvious from (12) that for sufficiently weak noise

$$W_{ij} \ll \tau_{rel}^{-1} \quad (R_i \gg D) . \tag{13}$$

It is the inequality (13) that makes the concept of transition probabilities sensible.

Fluctuational transitions give rise to fluctuations of the instantaneous populations $\tilde{w}_1(t)$, $\tilde{w}_2(t)$ of coexisting attractors. The kinetics of the populations is described by the balance equation.

$$\dot{\tilde{w}}_1(t) = -W_{12}\tilde{w}_1(t) + W_{21}\tilde{w}_2(t) ,$$
$$\tilde{w}_2(t) = 1 - \tilde{w}_1(t) \qquad (14)$$

The interwell fluctuations become pronounced in the range of parameters where the stationary values of the populations, w_1 and w_2, are of the same order of magnitude (obviously, because otherwise a system spends practically all its time near one of the attractors). This parameter range is quite narrow for weak noise, since according to (14) the ratio of the stationary populations,

$$w_1/w_2 = W_{21}/W_{12} = \text{const.} \times \exp[(R_1 - R_2)/D] , \qquad (15)$$

is either exponentially large or small: for most parameter values, $|R_1 - R_2| \gg D$ at small D (cf. (13)). The region where $R_1 \approx R_2$ can reasonably be called the range of a kinetic phase transition, by analogy with first-order phase transitions in thermal equilibrium systems where the populations of the phases (e.g. molar volumes, for a liquid–vapour transition) are of the same order of magnitude.

The fluctuations of the populations cause large (of the order of the distance between the attractors) fluctuations of the coordinate, momentum, amplitude of forced vibrations, etc. It would be expected therefore that, in the region of a kinetic phase transition, there will arise very intense and very narrow (with a width of the order of the transition probability) peaks in the SDFs of bistable systems [42] (similar peaks in susceptibilities were considered in [4]; cf. also [43]). In the case of bistability displayed in a periodic field with frequency ω_F, such supernarrow fluctuational-transition-induced peaks are positioned at ω_F and its overtones $n\omega_F$, including $n = 0$; those in the SDF of the coordinate of the bistable system are described by the expression [42]

$$Q_{\rm tr}^{(n)}(\omega) = \frac{1}{\pi} \frac{w_1 w_2 |q_1(n) - q_2(n)|^2 W}{W^2 + (\omega - n\omega_F)^2} ,$$
$$|\omega - n\omega_F| \ll \tau_{\rm rel}^{-1} ,$$
$$W = W_{12} + W_{21} . \qquad (16)$$

Here, $q_j(n)$ is the value of the nth Fourier component of the coordinate for the attractor j: because of the periodicity of the forced vibrations, the coordinate $q(t)$ for the jth attractor can be expanded as

$$[q(t)]_j = \sum_{n=-\infty}^{\infty} q_j(n) \exp(in\omega_F t) . \qquad (16a)$$

(in practice, for finite noise intensities, $q_j(n)$ differ slightly from their zero-noise values; this difference is neglected in what follows). We note that, for the particular case of an overdamped system performing Brownian motion in a static bistable potential, an expression of the type (16) (with $n = 0$) was given in [44]; the supernarrow zero-frequency peak was considered also in [24, 25, 45].

A supernarrow peak at the frequency of a driving periodic field was observed and the variation of its intensity with the parameters of the system was investigated in [46]. The system analysed was an analogue electronic model of an underdamped single-well Duffing oscillator described by (1), (7) with $\lambda = 0$, and the driving field $F \cos(\omega_F t)$ was nearly resonant, $|\omega_F - \omega_0| \ll \omega_F$. This system is closely related in particular to the case of a relativistic electron in a Penning trap: the motion of such an electron displays bistability in a sufficiently strong field with a frequency close to the cyclotron frequency [36]. The sharp onset of the supernarrow peak with variation of the dimensionless field intensity β,

$$\beta = 3F^2/32\omega_F^3|\omega_F - \omega_0|^3 \qquad (17)$$

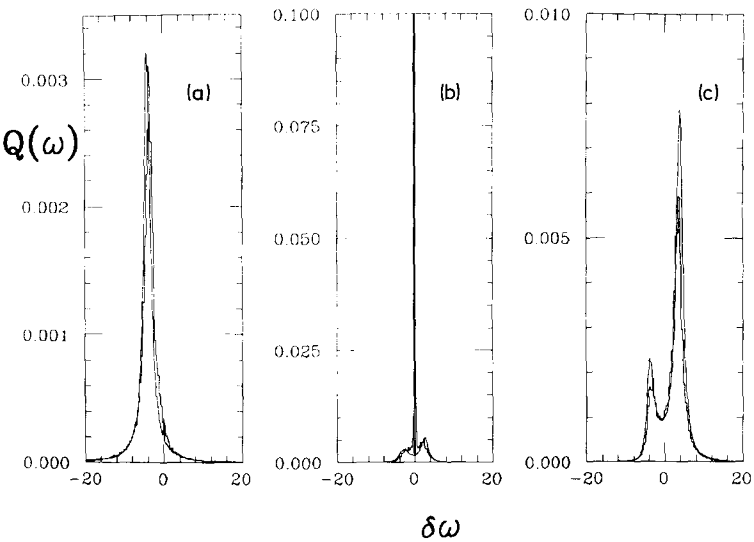

Fig. 8. Spectral densities $Q(\omega)$ of the fluctuations of the oscillator (1), (7) with $\lambda = 0$ driven by a strong, nearly resonant, periodic force $F\cos(\omega_F t)$, plotted as a function of $\delta\omega = (\omega_F - \omega_0)/\Gamma$ for three values of the dimensionless field intensity: (a) $\beta = 0.048$; (b) 0.078; (c) 0.150. The histograms are measurements from the electronic model, and the full curves are theoretical predictions [46]. The supernarrow spectral peak appears at $\delta\omega = 0$ in (b).

is shown in fig. 8. The width of the peak could not be resolved. The critical dependence of the intensity of the peak on the distance (in parameter space) to the phase-transition point is clearly evident in fig. 9. The full curves correspond to the expression

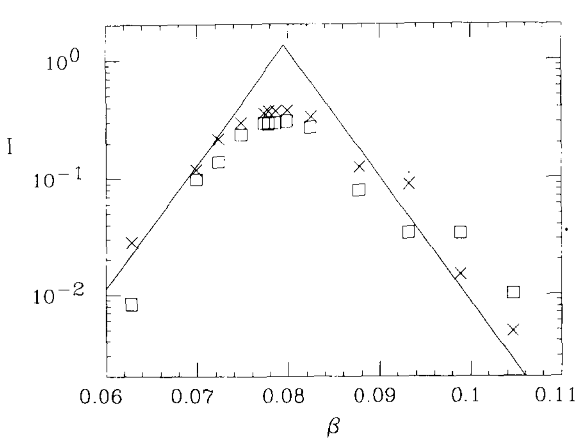

Fig. 9. Variation of the intensity I of the supernarrow peak with distance from the kinetic phase transition [46]. The square data points represent direct measurements. The crosses are theoretical values calculated from *measured* transition rates, and the full lines represent (18).

$$\ln(w_1 w_2) \simeq -|R_1' - R_2'|\,|\beta - \beta_c|/D\,, \tag{18}$$

which gives the logarithm of the intensity of the peak (16) with account taken of (15). The quantities R_1', R_2' in (18) are the derivatives of the transition activation energies (cf. (12)) with respect to the controlling parameter β, evaluated at the phase-transition point β_c; they were determined quite independently from measurements of the transition probabilities. The data clearly demonstrate that the experimental results are self-consistent and also provide some insight into the origin of the supernarrow peak.

A related problem of considerable interest is that of the influence of the characteristics of the noise on the supernarrow peaks. The only such characteristics entering the expression for the peak shape (16) are the transition probabilities that, from (12), seem to depend on the noise only in terms of its intensity (for Gaussian noise). However, the values of the activation energies are highly sensitive to the shape of the power spectrum of the noise [37–41] and, by varying this shape, one can not only produce marked changes in R_1, R_2, but also shift the position of the phase-transition point.

We note in conclusion of this section that the supernarrow peaks in the SDF's and the susceptibilities of bistable systems, in particular systems displaying bistability in a strong periodic field, are not only of interest as a means of studying kinetic critical phenomena e.g. in revealing the phase transition itself; they also provide a basis for the tunable filtering and detection of weak periodic signals.

4. Stochastic resonance in bistable systems: linear and nonlinear effects

An important phenomenon inherent to fluctuating bistable systems, one that occurs in the range of the kinetic phase transition, is stochastic resonance (SR). In fact, there are two distinct groups of phenomena both called SR. Originally [5], the term was used of periodically driven bistable systems to describe the dome-like (bell-shaped), seemingly resonant, dependence on noise intensity of the depth of the periodic modulation [4] of the instantaneous populations $\tilde{w}_1(t)$, $\tilde{w}_2(t)$ of the stable states. The other, more general, perception of SR [7] (which includes the first type of SR as a subset) is simply as the increase and subsequent decrease with increasing noise intensity of the response to a periodic field, i.e. of the susceptibility of the system. Viewed in the latter way, SR is no longer restricted to bistable systems, but can arise in monostable ones as well, as has been demonstrated very recently [47].

In what follows, however, we concentrate on SR in bistable systems and we consider the phenomena associated with the modulation of the instantaneous populations of the stable states. It is clear that this modulation will give rise, in turn, to a strong modulation of the coordinates, momenta, and other dynamic characteristics, i.e. it represents a strong overall response of the system to the field. Of course, the effect will only come into play when the noise intensity is large enough for transitions to occur between the stable states: thus, the effect can be promoted by noise and, consequently, in a certain interval of noise intensity, the coherent periodic response of the system *increases* with increasing noise. It is also evident that, being associated with the redistribution over the wells, SR is closely related to the onset of the supernarrow peaks considered in the preceding section.

There are several physical observables displaying an SR-type dependence on noise (cf. refs. [4–7, 11, 12, 48]). We shall analyse first a (slightly modified compared to (4)) SDF of a bistable system driven by trial field. It follows from the general concepts of statistical physics [1] that the average value of the coordinate of a system driven by a periodic force $A\cos(\Omega t)$ oscillates with the period $2\pi/\Omega$:

$$\langle q(t)\rangle = \sum_{n=0}^{\infty} a(n)\cos(n\Omega t + \phi(n)) \tag{19}$$

(if the system is driven by two fields there are terms in (19) with both frequencies, and also with their combinations: see below). It is clear from (19) that if we define the SDF of the coordinate as

$$S(\omega) = \lim_{t_0\to\infty} (4\pi t_0)^{-1} \left| \int_{-t_0}^{t_0} \mathrm{d}t\, q(t)\exp(\mathrm{i}\omega t)\right|^2 \tag{4a}$$

it will contain δ-shaped peaks at the frequency Ω and its overtones. The intensity S_n (total area) of the peak at the frequency $n\Omega$ is

$$S_n = \tfrac{1}{4}a^2(n)\,. \tag{20}$$

It was suggested in [7] that SR could conveniently be characterized by the ratio ρ of the trial-field-induced spike in $S(\omega)$ at the frequency Ω to the value $Q(\Omega) = S(\Omega)$ of the SDF in the absence of trial field,

$$\rho = S_1/Q(\Omega) \tag{21}$$

(the so-called signal-to-noise-ratio). It is quite straightforward to determine this ratio experimentally and it provides an important measure of the system's response to a trial field.

4.1. Linear response approximation

The easiest way to gain insight into SR and to find ρ is based on the fact that, for sufficiently weak trial fields (see below), the amplitudes of the harmonics $a(n)$ in (19) decrease very rapidly with increasing n so that, to a good approximation, it suffices to allow for the forced oscillations at the frequency Ω only, i.e., to retain in (19) only the terms with $n = 0, 1$. The term with $n = 0$ describes the time-independent part of $\langle q(t)\rangle$, and it remains unchanged to first order in the field amplitude; the main effect of the weak field is the onset of the term with $n = 1$. Taking account only of these two terms constitutes the linear response approximation [1]. The linear response is fully characterised by a susceptibility $\chi(\omega)$ [1, 49]:

$$a(1) = A|\chi(\Omega)|\,, \quad \rho = \tfrac{1}{4}A^2|\chi(\Omega)|^2/Q(\Omega)\,, \tag{22}$$

$$\phi(1) \equiv \phi = -\arctan[\mathrm{Im}\,\chi(\Omega)/\mathrm{Re}\,\chi(\Omega)]\,.$$

The susceptibility $\chi(\omega)$ can be calculated analytically for some simple model systems [4, 8, 10, 50]. It should be noted, however, that there is a broad class of systems of interest where $\chi(\omega)$ can be obtained from experimental measurements of the SDF in the *absence* of periodic driving, while a simple-minded analytical theory works only for a narrow range of parameters. This is the class of systems which are in thermal equilibrium (or quasiequilibrium). If a perturbing field is potential, i.e., its effect on a system can be determined by an extra term $-Aq\cos(\Omega t)$ in the Hamiltonian of the system, $\chi(\omega)$ can be expressed in terms of $Q(\omega)$ via the fluctuation-dissipation relations:

$$\mathrm{Re}\,\chi(\omega) = \frac{2}{T}\int_0^\infty d\omega_1\, Q(\omega_1)\,\omega_1^2(\omega_1^2-\omega^2)^{-1}\,,$$

$$\mathrm{Im}\,\chi(\omega) = \frac{\pi\omega}{T}\,Q(\omega)\,, \tag{23}$$

where the bar on the integral implies that we should take the Cauchy principal part. Some experimental data demonstrating, on one hand, the onset of SR in the signal-to-noise ratio ρ, and, on the other hand, the applicability of the relations (23) are shown in fig. 10. They refer to a Brownian "particle" (1) fluctuating in a symmetric double-well potential

$$U(q) = -\tfrac{1}{2}q^2 + \tfrac{1}{4}q^4\,. \tag{24}$$

The two sets of data were obtained from an analogue electronic circuit [51] simulating (1), (24) in two different ways: first (squares) by measuring ρ directly for the periodically driven system; and secondly (pluses) by making use of the measured $Q(\omega)$ obtained in the absence of periodic driving and of eqs. (22), (23). It is

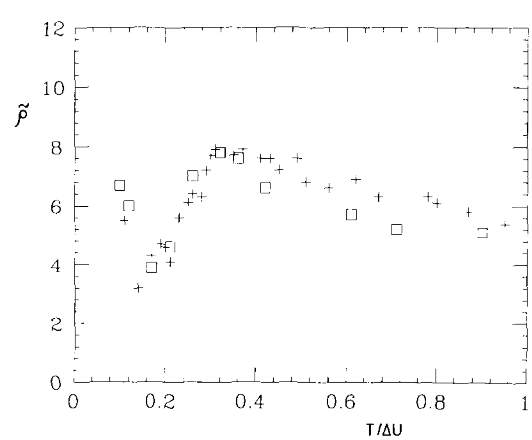

Fig. 10. Stochastic resonance [10]: the signal/noise ratio $\tilde{\rho} = 1.54 \times 10^3\rho$, defined by (21), measured for an electronic model of the oscillator (1), (24) driven by a weak periodic field, is plotted as a function of reduced noise intensity $T/\Delta U$. The square data points are direct measurements; the crosses are derived from (22), (23), based on measurements of the SDF in the *absence* of the periodic force. There are no adjustable parameters.

immediately evident from fig. 10 that ρ has a distinct maximum as a function of the noise intensity T thus demonstrating stochastic resonance, and also that the two ways of obtaining ρ give identical results.

Explicit expressions for $Q(\omega)$ and $\chi(\omega)$ for a Brownian particle (1) fluctuating in a bistable potential $U(q)$ can be obtained in the range of relatively small noise intensities,

$$T \ll \Delta U_1, \Delta U_2 ,$$
$$\Delta U_i = U(q_s) - U(q_i) \quad (i = 1, 2) , \tag{25}$$

where $q_{1,2}$ are the positions of the minima of the potential $U(q)$ and q_s is that of the local maximum, so that $U'(q_{1,2}) = U'(q_s) = 0$, $q_1 < q_s < q_2$. In this range, $Q(\omega)$ and $\chi(\omega)$ are given [42] by the sums of the "partial" contributions from fluctuations about the equilibrium positions $q_{1,2}$ and those from interwell transitions:

$$Q(\omega) = \sum_{i=1,2} w_i Q_i(\omega) + Q_{\mathrm{tr}}^{(0)}(\omega) ,$$
$$\chi(\omega) = \sum_{i=1,2} w_i \chi_i(\omega) + \chi_{\mathrm{tr}}^{(0)}(\omega) . \tag{26}$$

In eq. (26) w_i are the stationary populations of the stable states 1, 2 (cf. eqs. (14), (15)). The partial spectra $Q_i(\omega)$ in the low-noise range (25) for underdamped systems at ω close to $(U''(q_i))^{1/2}$ are given by eq. (6), while in the range of interest for SR, $\omega \leq (U''(q_i))^{1/2}$,

$$Q_i(\omega) = 2\Gamma T/\pi U_i''^2 + Q_{i0}(\omega), \quad U_i'' \equiv U''(q_i) ,$$
$$\Gamma, \omega \ll (U_i'')^{1/2} . \tag{27}$$

Here, $Q_{i0}(\omega)$ is the zero-frequency peak due to the local asymmetry of the potential about the bottom of the ith well; it is described by the expression (11) for $Q_0(\omega)$, with q_0', q_0'' calculated for the corresponding well. Alternatively, for overdamped systems,

$$Q_i(\omega) = 2\Gamma T/\pi(U_i''^2 + 4\Gamma^2\omega^2) , \quad \Gamma \gg (U_i'')^{1/2} \tag{27a}$$

(a more detailed expression that allows for the corrections $\sim T/\Delta U_i$ is given in [50]). The expression for the interwell-transition-induced contribution $Q_{\mathrm{tr}}^{(0)}(\omega)$ in (26) is given by eq. (16); only the term with $n = 0$ in (16) contributes to (26) in the particular case under consideration. The values of the "partial" susceptibilities $\chi_i(\omega)$ and of the interwell-transition-induced term $\chi_{\mathrm{tr}}^{(0)}(\omega)$ in the susceptibility are expressed in terms of $Q_i(\omega)$, $Q_{\mathrm{tr}}^{(0)}(\omega)$ by the relations (23).

The expressions (16), (26), (27), (27a) explain (cf. also [52]) the dependence of ρ on T plotted in fig. 10: for very small noise intensities the inequality $W \ll \Omega$ holds, and the interwell transitions contribute neither to the SDF nor to the susceptibility so that, according to (23), (27), (27a) ρ decreases roughly as T^{-1} with increasing T. This is because the partial spectra $Q_i(\omega)$ are proportional to T, whereas the susceptibilities $\chi_i(\omega)$ are seen from (23) to be T-independent. The increase of ρ starts for those T where W becomes of order of Ω. In the range where the interwell-transition-induced terms are dominant both in the SDF and susceptibility, one arrives at the simple expression

$$\rho = \tfrac{1}{4}\pi A^2 w_1 w_2 W(q_1 - q_2)^2/T^2 ,$$
$$W = W_{12} + W_{21} ,$$
$$Q_{\mathrm{tr}}^{(0)}(\omega) \gg Q_{1,2}(\omega) , \quad |\chi_{\mathrm{tr}}^{(0)}(\omega)| \gg |\chi_{1,2}(\omega)| . \tag{28}$$

It is seen from (12), (18), (28) that the dependence of the signal-to-noise ratio on the noise intensity is of the activation type, $\rho \propto \exp(-\Delta U_{\max}/T)$ where $\Delta U_{\max}$ is the depth of the deeper well.

Because the onset of SR is related to the supernarrow interwell-transition-induced peak, a strong amplification of the response to a weak trial periodic field would be expected to occur (for the present case of motion in a static potential) at comparatively small frequencies where the supernarrow peak at zero frequency can dominate the SDF:

$$\Omega \ll \Gamma, (U''_{1,2})^{1/2} . \tag{29}$$

The dependence of ρ on T for the range of the parameters outside the restrictions in (28) is still greatly simplified (compared to that given by (23), (27a)) for the particular situation of overdamped motion in a symmetric double-well potential,

$$U(q) = U(-q) , \quad 2\Gamma \gg (U'')^{1/2} \quad (U'' \equiv U''(q_{1,2})) . \tag{30}$$

In this case, for sufficiently small frequencies,

$$\rho = (\pi A^2/4T)(f^2U''^2 + \Omega^2)/(fU''^2 + 2\Gamma\Omega^2) , \quad f = (q_2 - q_1)^2 W/4T , \quad \Omega, W, [T/2\Gamma(q_2 - q_1)^2] \ll U''/2\Gamma , \tag{31}$$

For the same model, and in the same range of parameters, the phase shift between the signal $\langle q(t) \rangle$ and the driving force

$$\phi = -\arctan[(\Omega/U'') \times (fU''^2 + 2\Gamma\Omega^2)/(fWU'' + \Omega^2)] . \tag{32}$$

According to (31) the signal-to-noise ratio is minimal for the value of T given by the expression $fU'' \cong \Omega$, and it increases rapidly for higher T(cf. (28)). The maximum of ρ vs. T is reached in the region $T \sim \Delta U$, which is not described by the above analytic expressions for $Q(\omega)$, $\chi(\omega)$, but is still described by the fluctuation–dissipation relations.

It is evident from (32) that the phase shift also displays an SR-type behaviour [50]. From physical intuition, we may expect ϕ to provide a measure of the extent to which the external field is absorbed by the system. For very small noise, where the interwell transitions do not come into play, it follows from (32) that $|\phi| = 2\Gamma\Omega/U''$ is also very small: intrawell absorption of a low-frequency field is weak (the absorption band is broad, with the width $U''/2\Gamma \gg \Omega$). The increase of $|\phi|$ with T starts, however, for quite small T where ρ is still decreasing; $|\phi|$ reaches its maximum value when $T = T_{max}$ is still small compared with ΔU:

$$(-\phi)_{max} = \arctan(\tfrac{1}{2}[(q_2 - q_1)^2 U''/4T_{max}]^{1/2}) , \quad W(T_{max}) = \Omega[4T_{max}/(q_2 - q_1)^2 U'']^{1/2} . \tag{33}$$

It can be seen from (33) that $|\phi|_{max}$ is quite large, i.e., there then is a strong absorption of the periodic field. This absorption is due primarily to the interwell transitions. We note that the absorption coefficient itself, which is proportional to Im $\chi(\Omega)$, also displays an SR-type behaviour. Both $|\phi|$ and Im $\chi(\Omega)$ are much steeper on the small-T side of their maxima, because it is the activation dependence of the transition probabilities on T that determines the behaviour of $\chi(\Omega)$ in this range.

The stochastic-resonance-like dependence of the phase shift upon noise intensity has been clearly demonstrated in analogue electronic experiments [50]. Some data for an overdamped

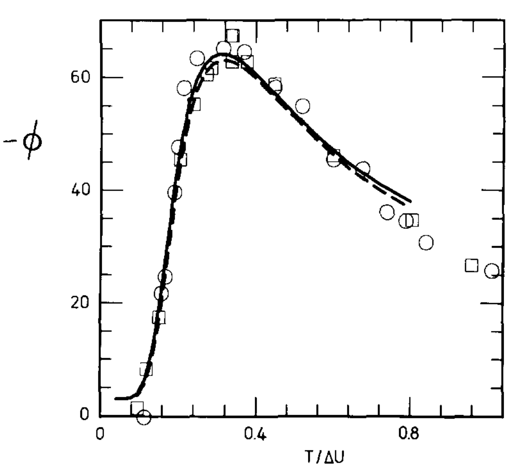

Fig. 11. The phase shift $-\phi$ (degrees) between the weak periodic force $A \cos \Omega t$ and the averaged coordinate $\langle q(t) \rangle$, measured for an electronic model of the overdamped oscillator described by (1), (24), (3) with $\Omega = 0.1$ for $A/2\Gamma = 0.04$ (circle data points) and $A/2\Gamma = 0.2$ (squares). The dashed curve represents the simple linear response prediction (31); the full curve takes account of nonlinear corrections for $A/2\Gamma = 0.04$ [50].

oscillator with the potential (24) are shown in fig. 11. The simple expression (31) is evidently in excellent agreement with the experimental data (the prefactor in the expression (12) for the transition probability of an overdamped system was taken to be of the standard form [29]); the comparison of theory with experiment does not involve any adjustable parameters.

4.2. Nonlinear effects

One of the more intriguing features of the response of a bistable system to a low-frequency field (the effects for high-frequency fields will be considered below) is the possibility of observing strongly nonlinear effects, even for small field amplitudes A. Such a possibility arises because the field-induced modulation of the populations of the attractors comes about primarily through a modulation of the activation energies of fluctuational transitions; and the effect of the latter modulation is enhanced exponentially, because it is with the small noise intensity that this modulation should be compared (cf. (12)). It is seen from the expressions (15) that the parameter g describing the redistribution over the attractors is of the form

$$g = \frac{A}{D}\left|\frac{\partial}{\partial A}[R_1(A) - R_2(A)]\right|_{A=0} . \tag{34}$$

Here, $R_i(A)$ is the activation energy of the transition from the state i for the initial system driven additionally by a weak force A, and the derivatives are calculated for $A = 0$ (see [10a]; the importance of a parameter of this kind was also recognised recently in [11]). The variation of R_1, R_2 under the weak force A is assumed small: accordingly, only terms of the first order in A will be taken into account in $R_i(A)$.

In considering nonlinear effects we shall assume the field $A\cos(\Omega t)$ to be slowly varying, $\Omega \ll U''/2\Gamma, \Gamma$ (cf. (31)), so that the transition probabilities can be considered in the adiabatic approximation. In this case their values depend on the instantaneous value of the field as they would if it were a fixed parameter. Then according to (12) the instantaneous transition probability $\tilde{W}_{ij}(t)$ is given by the expression

$$\tilde{W}_{ij}(t) = W_{ij} \sum_{k=-\infty}^{\infty} I_k(g_i)\exp(\mathrm{i}k\Omega t) ,$$
$$g_i = -\frac{A}{D}\left(\frac{\partial R_i}{\partial A}\right)_{A=0} , \tag{35}$$

where W_{ij} are the values of the transition probabilities in the absence of the field, i.e., for $A = 0$; I_k are modified Bessel functions [53]. The periodic dependence of the transition probabilities on time, which is strongly nonsinusoidal for $|g_i| > 1$, gives rise to the nonsinusoidal time dependence of the instantaneous state populations $\tilde{w}_{1,2}(t)$. Eqs. (14), (35) result in the following set of linear algebraic equations for the Fourier components $\tilde{w}_{1k}$:

$$\tilde{w}_1(t) = \sum_{k=-\infty}^{\infty} \tilde{w}_{1k}\exp(\mathrm{i}k\Omega t) ,$$
$$[\mathrm{i}k\Omega + W_{12}I_0(g_1) + W_{21}I_0(g_2)]\tilde{w}_{1k} + \sum_{s\neq 0}[W_{12}I_s(g_1) + W_{21}I_s(g_2)]\tilde{w}_{1k-s} = W_{21}I_k(g_2) . \tag{36}$$

It is straightforward to express the amplitudes $a(k)$ and phases $\phi(k)$ of the forced vibrations of the system (cf. eq. (19)) in terms of $\tilde{w}_{1k}$. For $k > 1$,

$$a(k) = 2|(q_1 - q_2)\tilde{w}_{1k}| ,$$
$$\phi(k) = \arg[(q_1 - q_2)\tilde{w}_{1k}] \quad (k > 1) , \tag{37}$$

while the expressions for $a(1)$, $\phi(1)$ are of the form (22) with the susceptibility $\chi(\Omega)$ having been replaced by $\tilde{\chi}(\Omega)$:

$$\tilde{\chi}(\Omega) = \tilde{w}_{10}\chi_1(\Omega) + (1 - \tilde{w}_{10})\chi_2(\omega) + 2A^{-1}w^*_{11}(q_1 - q_2) . \tag{38}$$

Eqs. (35)–(38) make it straightforward to compute the response to a slowly varying field for arbitrary nonlinearity. They obviously go over into the results of linear-response theory in the limit of weak field where $|g_{1,2}| \ll 1$.

The extreme nonlinear case $|g_{1,2}| \gg 1$ can be also analysed analytically, by application of a quite different approach [10a]. In this case inter-well transitions from the state i, for example, happen, with an overwhelming probability during that part of the period of the driving field $2\pi/\Omega$ where the activation energy $R_i(A)$ is minimal, i.e., the field works as a shutter (we stress that the field itself is weak; this is not a deterministic, but a probabilistic shutter). As a result, the average signal at the output will be rectangular. In particular, in the case of Brownian motion in a symmetric double-well potential (30) in the neglect of intrawell contributions,

$$\langle q(t) \rangle = 2\bar{q} \sum_{n=-\infty}^{\infty} \left[\Theta\left(t - \frac{2\pi n}{\Omega}\right) - \Theta\left(t - \frac{\pi(2n+1)}{\Omega}\right)\right] - \bar{q} ,$$

$$\bar{q} = -q_1 \tanh \bar{g} ,$$

$$\bar{g} = \left(\frac{2\pi T}{|Aq_1|}\right)^{1/2} \frac{W_{12}}{2\Omega} \exp(|Aq_1|/T) , \qquad (39)$$

where $\Theta(t)$ is the unit step-function. We note that the "amplitude" $\bar{q}$ of the rectangular wave (39) saturates quite quickly as a function of $\bar{g}$ (starting with $\bar{g} \gtrsim 1.5$), and therefore the intensities of the spectral peaks in the SDF $S(\omega)$ as defined by (4a) depend only weakly on the field amplitude A.

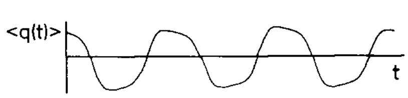

Fig. 12. The averaged coordinate $\langle q(t) \rangle$ measured for an electronic model [50] of the overdamped oscillator (1), (24), (30), driven by a periodic force $A \cos \Omega t$ with $A/2\Gamma = 0.1$, $T/2\Gamma = 0.0644$, for a very low frequency $\Omega = 1.9 \times 10^{-5}$. As predicted theoretically (39), the result approximates a square wave. Its tops and bottoms are curved due to intra-well vibrations, and tilted due to the phase shift between the latter and the inter-well transitions.

The nearly rectangular signal under sinusoidal driving by a slowly varying field has been observed in an analogue electronic experiment [50]. The result is shown in fig. 12. The distortion of the signal is related to the contribution of the forced intrawell vibrations. We stress that the periodic driving force was itself comparatively weak, so that the nonlinearity of this effect is indeed quite remarkably strong.

4.3. "Nonconventional" stochastic resonance

Until recently, stochastic resonance was considered purely as an effect that arises for Brownian motion in a static bistable potential with a superimposed slowly varying field (cf. [5–12, 50, 52]). It follows from the above formulation, however, that it is actually a quite general phenomenon for fluctuating bistable systems in the range of a kinetic phase transition. Consequently, it may also be expected to occur for systems displaying bistability under strong periodic driving [46] (the onset of a large susceptibility with respect to an additional weak trial field was predicted for systems of just this kind in [4]). In this latter case SR will be inherent to the response, not only to a low-frequency, but also to a high-frequency field [54]. Also, since bistable systems are strongly nonlinear, periodic driving of various parameters (not only of their coordinates or momenta) can also give rise to a periodic signal (i.e. to periodic variation of the coordinate), and in some cases this signal can display a dome-like dependence on the noise intensity. One such parameter could be the noise intensity itself [55]. The results for these two new types of SR are described briefly below.

First, we consider high frequency stochastic resonance for periodic attractors. As pointed out above, the onset of SR is related to a comparatively strong noise-enhanced modulation of the populations of the attractors $\tilde{w}_1(t)$, $\tilde{w}_2(t)$ by a trial field. Since the characteristic time-scale for the variation of the populations is given by the reciprocal transition probabilities, the modulation can be effective provided it is slow. A feature of nonlinear systems is that they perform mixing of the frequencies of external fields. Therefore, if a system is driven by a (strong) field $F\cos(\omega_F t + \phi_F)$ and a (weak) trial field $A\cos(\Omega t)$ then the variables of the system will oscillate at combination frequencies $|\pm n\omega_F + \Omega$ ($n = 0, 1, 2, \ldots$) and thus if one of these is small the corresponding oscillations can give rise to effective redistribution over the attractors.

The simplest case is just $|\omega_F - \Omega| \ll \tau_{rel}^{-1}$. The dynamics of the system in this case can be considered as that in the strong field $\mathrm{Re}[F(t)\exp(i\omega_F t + i\phi_F)]$, but with the complex amplitude $F(t)$ slowly varying in time,

$$F(t) = F + A\exp[i(\Omega - \omega_F)t - i\phi_F]\,. \tag{40}$$

The activation energies $R_{1,2}$ of the transitions between the attractors depend on F (strictly, on F^2, since they are determined by the intensity rather than by the fast oscillating phase of the field). For small $|\Omega - \omega_F|$, they get modulated at frequency $|\Omega - \omega_F|$ and, for a sufficiently weak trial field, R_i in the expression (12) should be replaced by $\tilde{R}_i(t)$,

$$\tilde{R}_i(t) = R_i + \frac{\partial R_i}{\partial F^2}\,2AF\cos[(\Omega - \omega_F)t - \phi_F]\,. \tag{41}$$

The further analysis of the redistribution over the attractors is closely similar to that in the preceding subsection. It should be stressed, however, that the modulation of the populations of the attractors at frequency $|\Omega - \omega_F|$ gives rise to periodic oscillations, not only at the trial-field frequency Ω, but also at the mirror-reflected frequency $|2\omega_F - \Omega|$. For small A, where the linear-response approximation holds, the trial-field-induced addition to the average value of the coordinate is of the form

$$\delta\langle q(t)\rangle = A\,\mathrm{Re}\{\chi(\Omega)\exp(-i\Omega t) + \bar{\chi}(\Omega) \times \exp[-i(2\omega_F - \Omega)t]\}\,. \tag{42}$$

In the case of weak noise, the susceptibilities $\chi(\Omega)$, $\bar{\chi}(\Omega)$ can be written in the form (26), and the transition-induced contributions are of the form

$$\begin{aligned}\chi_{tr}(\Omega) &= \frac{2F}{D}\,w_1 w_2[q_1^*(1) - q_2^*(1)] \\ &\quad\times \frac{\partial(R_1 - R_2)}{\partial F^2}\,\frac{W}{W - i(\Omega - \omega_F)}\,, \\ \bar{\chi}_{tr}(\Omega) &= \chi_{tr}(2\omega_F - \Omega)\exp(-2i\phi_F)\,.\end{aligned} \tag{43}$$

Both of them display SR.

High-frequency stochastic resonance (HFSR) of this type has been observed for periodic attractors in analogue electronic experiments [54]. The system simulated was the one already discussed above in section 3: an underdamped nonlinear oscillator with a single-well potential given by eq. (7) with $\lambda = 0$, which has two types of coexisting vibrational states under a sufficiently strong nearly resonant field. When the oscillator was driven, in addition, by a trial field of frequency $\Omega \cong \omega_F$ there occurred two clearly resolved extra δ-shaped spikes in the SDF of the coordinate $S(\omega)$. The dependence of the intensity of these spikes on the noise intensity can be seen from fig. 13 to be just of the SR-type. The theoretical curves are based on measured values of the activation energies of the transitions (cf. fig. 9); the experimental uncertainty arising from the latter data is shown by the bars. Given the large systematic errors inherent in these measurements – arising e.g. from β (17) which contains the small difference between two large quantities $|\omega_F - \omega_0|$ raised to its third power – the agreement can be regarded as very satisfactory; in particular, the theoretical and experimental curves are of a similar shape, and their maxima lie at nearly the same T. Fig. 14 demonstrates that high-frequency SR is a purely critical phenomenon: the intensities of the spikes decrease exponentially as the control parameter β (17) moves away from its critical value. We note that these experiments are quite delicate, since an extremely high resolution is necessary to

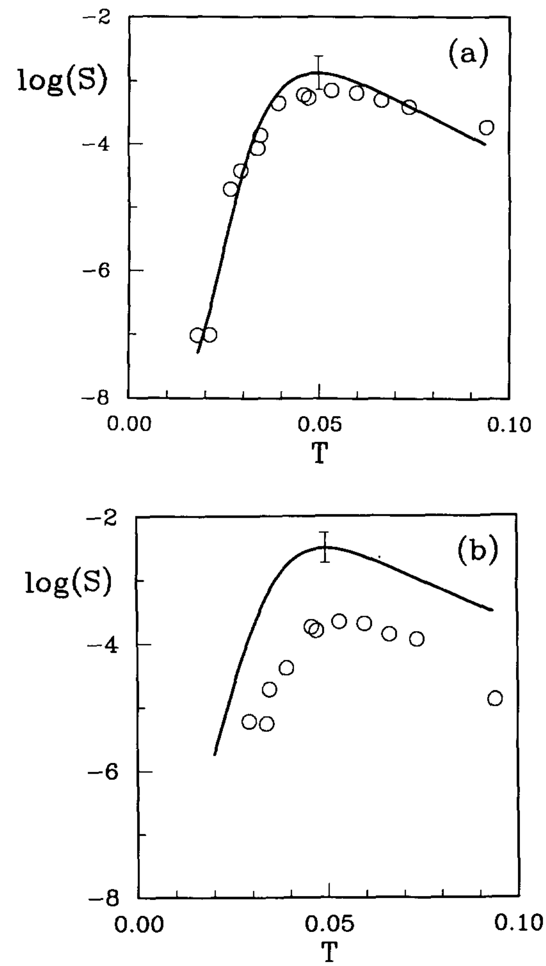

Fig. 13. High frequency stochastic resonance for periodic attractors, measured for an electronic model of the oscillator described by (1), (7) with $\lambda = 0$, driven by a strong periodic field $F\cos(\omega_F t + \phi_F)$ and a weak trial force $A\cos\Omega t$ [54]. The logarithms of the intensities S of the δ-shaped spikes in the spectral density of the fluctuations (a) at frequency Ω and (b) at $2\omega_F - \Omega$ are plotted (data points) as a function of the noise intensity T. The curves are theoretical predictions based on *measured* values of the activation energies; they are subject to the systematic uncertainties indicated by the bars. There are no adjustable parameters.

observe and investigate the peaks, given that they must be separated by a frequency difference much smaller than the reciprocal relaxation time which, in its turn, is much smaller than the frequencies ω_F, Ω themselves.

The second nonconventional form of SR refers to physical situations where the noise and signal acting upon a system are not additive, but multiplicative: it is noise (or noise intensity) that is modulated directly by the signal, and it may be such a periodically modulated noise that drives the system itself. If the initial noise is of zero mean, the driving field will also be of zero mean. Nonetheless, a nonlinear system can still detect the modulating signal via nonlinear transformations. It is demonstrated below that, for bistable systems, the quality of detection may increase with increasing noise intensity and display an SR-type behaviour.

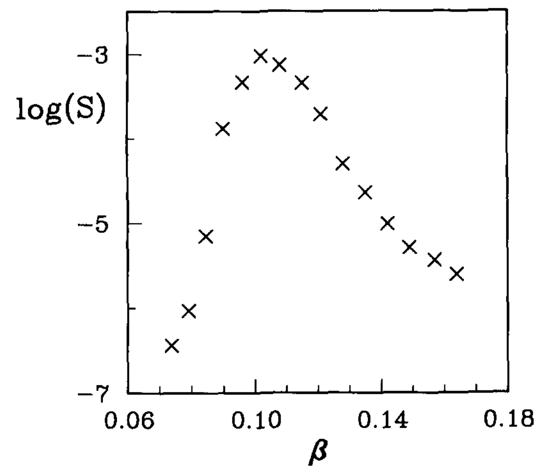

Fig. 14. The logarithm of the intensity S of the δ-shaped spike at frequency Ω in the spectral density of the fluctuations for high-frequency stochastic resonance [54], plotted as a function of the dimensionless field intensity β (17) which gives a measure of the distance from the kinetic phase transition line.

We shall consider SR in the response to modulated noise for the simplest bistable system: an overdamped particle oscillating in a bistable potential and described by the equation

$$2\Gamma\dot{q} + U'(q) = \xi(t)\,,$$
$$\xi(t) = [\tfrac{1}{2}A\cos(\Omega t) + 1]f(t)\,,$$
$$U(q) = -\tfrac{1}{2}q^2 + \tfrac{1}{4}q^4 + \lambda q\,,$$
$$\langle f(t)\, f(t')\rangle = 4\Gamma T\delta(t-t')\,. \tag{44}$$

In contrast to the former analysis it is the amplitude of the noise that is assumed to be periodically modulated here; the potential is assumed to be asymmetric, with the asymmetry parameter λ (the asymmetry turns out to be crucial for obtaining a well-pronounced SR).

If the amplitude A is sufficiently weak, we can characterise the response of the system to the corresponding modulation in terms of a generalised susceptibility $\aleph(\omega)$ and write the signal-induced term in the average value of the coordinate as

$$\delta\langle q(t)\rangle = A\,\mathrm{Re}[\aleph(\Omega)\exp(-\mathrm{i}\Omega t)]\,. \tag{45}$$

For weak noise intensities and for a slowly varying field, $\Omega \ll U''/2\Gamma$, the function $\aleph(\Omega)$ (just as for the "normal" susceptibility $\chi(\Omega)$) is a sum of contributions from the vibrations in the vicinities of the stable states q_1, q_2 and from the interwell transitions (cf. (26)):

$$\aleph(\Omega) = \sum_{i=1,2} w_i \aleph_i(\Omega) + \aleph_{\mathrm{tr}}(\Omega)\,. \tag{46}$$

The contribution from the interwell transitions, which is the one of primary interest, originates from the fact that the transition probabilities depend on the instantaneous value of the noise intensity (it varies slowly because of the modulation) and, provided that the potential is asymmetric so that $W_{12} \neq W_{21}$, the periodic variation of W_{ij} gives rise to a periodic change of the state populations; for a symmetric potential, the variation of the noise intensity does not break the symmetry, and so the populations remain equal. The resulting expression for $\aleph_{\mathrm{tr}}(\Omega)$ is of the form [55]

$$\aleph_{\mathrm{tr}}(\Omega) = -\frac{1}{T}\,\frac{(q_1 - q_2)(\Delta U_1 - \Delta U_2) w_1 w_2 W}{(W - \mathrm{i}\Omega)}\,. \tag{47}$$

Thus, a periodic signal will indeed occur under driving by a zero-mean periodically modulated noise for an *asymmetric* potential ($\Delta U_1 \neq \Delta U_2$); furthermore, the amplitude of the signal $|\aleph_{\mathrm{tr}}(\Omega)|$ is seen from (47) to increase sharply with the increasing noise intensity T.

The dependence of the signal-to-noise ratio, defined by analogy to (21) as the ratio of the δ-shaped spike in the SDF $S(\omega)$ at frequency Ω to the value of $S(\Omega) = Q(\Omega)$ in the absence of modulation, is shown in fig. 15: the theoretical prediction is compared with the results from an analogue electronic experiment (the lower full curve and square data points, respectively). The phenomenon of stochastic resonance is clearly evident in this situation, although slightly less pronounced than for "conventional" periodic driving (upper curve and circle data), i.e. driving the system rather than the noise. It is evident from the lower curve and data of fig. 16 that this type of SR is intimately connected with the asymmetry of the potential (44), i.e. with the finiteness of the parameter λ; for $\lambda = 0$ the signal could not be detected. At the opposite extreme for very strong asymmetry, there will again be no SR because in practice only one well will be populated for weak noise and the interwell tran-

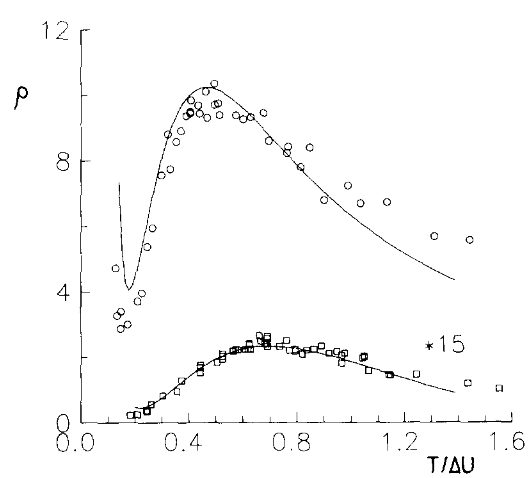

Fig. 15. Stochastic resonance for periodically modulated noise [55]. Measurements ($\times 15$) of the signal/noise ratio ρ defined by (21) for an electronic circuit model of (44) with $A = 0.14$, $\lambda = 0.2$, $\Omega = 0.029$ are plotted (data points) as a function of the reduced noise intensity $\Delta U = 1/4$; the full curve represents the theoretical prediction. The upper curve and circle data show the theory and measurements using the same circuit with *additive* periodic forcing (conventional stochastic resonance) under similar conditions (theoretical results are valid for $T \ll \Delta U_{1,2}$, strictly speaking).

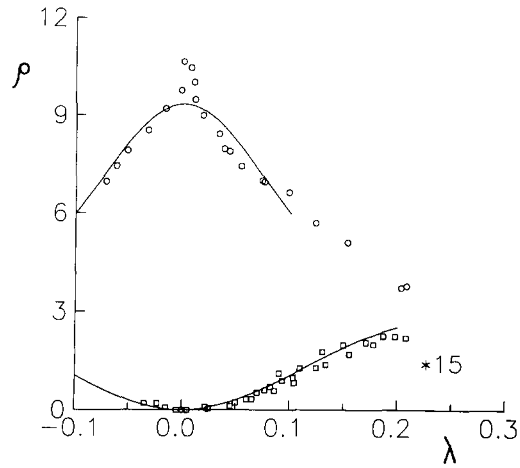

Fig. 16. Effect of the asymmetry parameter λ on stochastic resonance [55]. Measurements ($\times 15$) of the signal/noise ratio ρ defined by (21) for an electronic circuit model of (44) with $A = 0.15$, $(T/\Delta U)_{\lambda=0} = 0.303$, $\Omega = 0.029$ are plotted (square data points) as a function of λ; the full curve represents the theoretical prediction. The upper curve and circle data show the theory and measurements using the same circuit with *additive* periodic forcing (conventional stochastic resonance) under similar conditions.

sitions will be "frozen out". Therefore, in order to investigate SR under these conditions, it is necessary to optimise the asymmetry of the system.

5. Conclusions

It follows from the above results that the traditional field of noise-driven dynamics and, in particular, investigations of the spectral densities of fluctuations of noise-driven systems, is far from being exhausted. There still arise new and unexpected phenomena like the noise-induced narrowing of spectral peaks, the onset of extra peaks such as the zero-dispersion and supernarrow ones, and also stochastic resonance. All of these phenomena are very general. They are not "pinned" to particular models, and thus they are of fundamental interest. At the same time, they are also rich in potential applications, ranging from solid state physics, through electrons localised in Penning traps, to neurons and neural networks, as mentioned above. There still remain a number of significant problems that have not been solved, or even addressed. Many of these are related to the interplay of dynamical chaos and noise. We hope, therefore, that these investigations will continue, and that our understanding of noise-driven nonlinear dynamics will thereby be substantially enriched.

Acknowledgements

It is our great pleasure to acknowledge our indebtedness to those people in immediate collaboration with whom the above ideas have been worked out and the results obtained. These are the late M.A. Krivoglaz, D.G. Luchinsky, R. Mannella, S.M. Soskin, N.D. Stein and N.G. Stocks. The work has been supported by the Science and Engineering Research Council (UK).

References

[1] L.D. Landau and E.M. Lifshitz, Statistical Physics, 3rd ed. (Pergamon, New York, 1980), Part 1, revised by E.M. Lifshitz and L.P. Pitaevskii.

[2] A.S. Barker Jr. and A.J. Sievers, Rev. Mod. Phys. 47 Suppl. No. 2 (1975) S1.

[3] S.M. Soskin, Physica A 155 (1989) 401.

[4] (a) M.I. Dykman and M.A. Krivoglaz, Zh. Eksp. Teor. Phys. 77 (1979) 60 [Sov. Phys. JETP 50 (1979) 30]; (b) in: Soviet Physics Reviews, ed. I.M. Khalatnikov (Harwood, New York, 1984) Vol. 5, p. 265.

[5] R. Benzi, A. Sutera and A. Vulpiani, J. Phys. A 14 (1981) L453; R. Benzi, G. Parisi, A. Sutera and A. Vulpiani, Tellus 34 (1982) 10.

[6] C. Nicolis, Tellus 34 (1982) 1.

[7] B. McNamara, K. Wiesenfeld and R. Roy, Phys. Rev. Lett. 60 (1988) 2626.

[8] M.I. Dykman, A.L. Velikovich, G.P. Golubev, D.G. Luchinsky and S.V. Tsuprikov, JETP Lett. 53 (1991) 193.

[9] S. Fauve and F. Heslot, Phys. Lett. A 97 (1983) 5; L. Gammaitoni, F. Marchesoni, E. Menichella-Saetta and S. Santucci, Phys. Rev. Lett. 62 (1989) 349; G. Debnath, T. Zhou and F. Moss, Phys. Rev. A 39 (1989) 4323.

[10] (a) M.I. Dykman, P.V.E. McClintock, R. Mannella and N.G. Stocks, JETP Lett. 52 (1990) 141; (b) M.I. Dykman, R. Manella, P.V.E. McClintock and N.G. Stocks, Phys. Rev. Lett. 65 (1990) 2606.
[11] T. Zhou, F. Moss and P. Jung, Phys. Rev. A 42 (1990) 3161.
[12] A. Longtin, A. Bulsara and F. Moss, Phys. Rev. Lett. 67 (1991) 656.
[13] J.B. Morton and S. Corssin, J. Stat. Phys. 2 (1970) 153.
[14] M.A. Krivoglaz and I.P. Pinkevich, Ukr. Fiz. Zh. 15 (1970) 2039; Y. Onodera, Prog. Theor. Phys. 44 (1970) 1477.
[15] M.I. Dykman and M.A. Krivoglaz, Phys. Stat. Sol. (b) 48 (1971) 497.
[16] K. Sture, J. Nordholm and R. Zwanzig, J. Stat. Phys. 11 (1974) 143.
[17] R.F. Rodriguez and N.G. van Kampen, Physica A 85 (1976) 347.
[18] S.H. Crandall, in: Random Vibrations, ed. S.H. Crandall (MIT Press, Cambridge, MA, 1963), Vol. 2, p. 85.
[19] A.B. Budgor, K. Lindenberg and K.E. Shuler, J. Stat. Phys. 15 (1976) 375; A.R. Bulsara, K. Lindenberg and K.E. Shuler, J. Stat. Phys. 27 (1982) 787.
[20] M.I. Dykman and M.A. Krivoglaz, Physica A 104 (1980) 495.
[21] B. Carmeli and A. Nitzan, Phys. Rev. A 32 (1985) 2439.
[22] W. Renz, Z. Phys. B 59 (1985) 91; L. Fronzoni, P. Grigolini, R. Mannella and B. Zambon, J. Stat. Phys. 41 (1985) 553; Phys. Rev. A 34 (1986) 3293; W. Renz and F. Marchesoni, Phys. Lett. A 112 (1985) 124.
[23] J.J. Brey, J.M. Casado and M. Morillo, Physica A 123 (1989) 481.
[24] M.I. Dykman, R. Mannella, P.V.E. McClintock, F. Moss and S.M. Soskin, Phys. Rev. A 37 (1988) 1303.
[25] H. Risken, The Fokker–Planck Equation, 2nd ed. (Springer, Berlin, 1989).
[26] M.A. Ivanov, L.B. Kvashnina and M.A. Krivoglaz, Fiz. Tverd. Tela 7 (1965) 2047 [Soviet Phys. – Solid State 7 (1965) 1652].
[27] M.I. Dykman, R. Mannella, P.V.E. McClintock, S.M. Soskin and N.G. Stocks, Phys. Rev. A 42 (1990) 7041.
[28] B.P. Clayman, Phys. Rev. B 3 (1971) 2813.
[29] H.A. Kramers, Physica 7 (1940) 284.
[30] N.G. Stocks, P.V.E. McClintock and S.M. Soskin, Phys. Rev. A (1992).
[31] S.M. Soskin, Physica A 180 (1992) 386.
[32] R.J. Elliott, W. Hayes. G.D. Jones, H.F. McDonald and C.T. Sennett, Proc. R. Soc. A 289 (1965) 1.
[33] M.I. Dykman and M.A. Krivoglaz, Ukr. Fiz. Zh. 17 (1972) 1971.
[34] M.I. Dykman, R. Mannella, P.V.E. McClintock, S.M. Soskin and N.G. Stocks, Phys. Rev. A 43 (1991) 1701.
[35] M.A. Krivoglaz and I.P. Pinkevich, Zh. Eksp. Teor. Fiz. 51 (1966) 1151 [Sov. Phys. – JETP 24 (1966) 772].
[36] G. Gabrielse, H. Dehmelt and W. Kells, Phys. Rev. Lett. 54 (1985) 537.
[37] J.F. Luciani and A.D. Verga, Europhys. Lett. 4 (1987) 255; J. Stat. Phys. 50 (1988) 567.
[38] A.J. Bray and A.J. McKane, Phys. Rev. Lett. 62 (1989) 493; A.J. McKane, Phys. Rev. A 40 (1989) 4050; A.J. McKane, H.C. Luckock and A.J. Bray, Phys. Rev. A 41 (1990) 644.
[39] M.M. Klosek-Dygas, B.J. Matkowsky and Z. Schuss, SIAM J. Appl. Math. 48 (1988) 425; J. Stat. Phys. 54 (1989) 1309.
[40] H.S. Wio, P. Colet, M. San Miguel, L. Pesquera and M.A. Rodriguez, Phys. Rev. A 40 (1989) 7312.
[41] M.I. Dykman, Phys. Rev. A 42 (1990) 2020; M.I. Dykman, P.V.E. McClintock, N.D. Stein and N.G. Stocks, Phys. Rev. Lett. 67 (1991) 933.
[42] M.I. Dykman, M.A. Krivoglaz and S.M. Soskin, in: Noise in Nonlinear Dynamical Systems, eds. F. Moss and P.V.E. McClintock (Cambridge Univ. Press, Cambridge, 1989) Vol. 2, p. 347.
[43] M.R. Beasley, D. D'Humieres and B.A. Huberman, Phys. Rev. Lett. 50 (1983) 1328.
[44] P. Hanggi and H. Thomas, Phys. Rep. 88 (1982) 207.
[45] F.T. Arecchi and F. Lisi, Phys. Rev. Lett. 49 (1982) 94; 50 (1983) 1330; R.F. Voss, Phys. Rev. Lett. 50 (1983) 1329; F.T. Arecchi, R. Badii and A. Politi, Phys. Rev. A 32 (1985) 402; F.T. Arecchi and A. Califano, Europhys. Lett. 3 (1987) 5.
[46] M.I. Dykman, R. Mannella, P.V.E. McClintock and N.G. Stocks, Phys. Rev. Lett. 65 (1990) 48.
[47] N.G. Stocks, N.D. Stein and P.V.E. McClintock, Stochastic resonance in monostable systems, submitted to Phys. Rev. Lett.
[48] Hu Gang, G. Nicolis and C. Nicolis, Phys. Rev. A 42 (1990) 2030.
[49] R. Kubo, J. Phys. Soc. Jpn. 12 (1957) 570.
[50] M.I. Dykman, R. Mannella, P.V.E. McClintock and N.G. Stocks, Phys. Rev. Lett. 68 (1992) 2985; and to be published.
[51] P.V.E. McClintock and F. Moss, in: Noise in Nonlinear Dynamical Systems, eds. F. Moss and P.V.E. McClintock, (Cambridge, Univ. Press, Cambridge, 1989), vol. 3, p. 243.
[52] B. McNamara and K. Wiesenfeld, Phys. Rev. A 39 (1989) 4854.
[53] M. Abramovitz and I. Stegun, eds., Handbook of Mathematical Functions (Dover, New York, 1970).
[54] M.I. Dykman, R. Mannella, P.V.E. McClintock, N.D. Stein and N.G. Stocks, High-frequency stochastic resonance for periodic attractors, to be published.
[55] M.I. Dykman, D.G. Luchinsky, P.V.E. McClintock, N.D. Stein and N.G. Stocks, Stochastic resonance for periodically modulated noise intensity, submitted to Phys. Rev. A.